Interdiscip Sci Comput Life Sci
DOI 10.1007/s12539-016-0186-3

ORIGINAL RESEARCH ARTICLE

# Molecular Recognition of Azelaic Acid and Related Molecules with DNA Polymerase I Investigated by Molecular Modeling Calculations

**Jakaria Shawon[1,2] · Akib Mahmud Khan[1,2] · Adhip Rahman[1] · Mohammad Mazharol Hoque[1] · Mohammad Abdul Kader Khan[3] · Mohammed G. Sarwar[4] · Mohammad A. Halim[1,5]**

Received: 22 June 2016 / Revised: 20 August 2016 / Accepted: 12 September 2016


**Abstract** Molecular recognition has central role on the development of rational drug design. Binding affinity and interactions are two key components which aid to understand the molecular recognition in drug-receptor complex and crucial for structure-based drug design in medicinal chemistry. Herein, we report the binding affinity and the nonbonding interactions of azelaic acid and related compounds with the receptor DNA polymerase I (2KFN). Quantum mechanical calculation was employed to optimize the modified drugs using B3LYP/6-31G(d,p) level of theory. Charge distribution, dipole moment and thermodynamic properties such as electronic energy, enthalpy and free energy of these optimized drugs are also explored to evaluate how modifications impact the drug properties. Molecular docking calculation was performed to evaluate the binding affinity and nonbonding interactions between designed molecules and the receptor protein. We notice that all modified drugs are thermodynamically more stable and some of them are more chemically reactive than the unmodified drug. Promise in enhancing hydrogen bonds is found in case of fluorine-directed modifications as well as in the addition of trifluoroacetyl group. Fluorine participates in forming fluorine bonds and also stimulates alkyl, pi-alkyl interactions in some drugs. Designed drugs revealed increased binding affinity toward 2KFN. **A1**, **A2** and **A3** showed binding affinities of −8.7, −8.6 and −7.9 kcal/mol, respectively against 2KFN compared to the binding affinity −6.7 kcal/mol of the parent drug. Significant interactions observed between the drugs and Thr358 and Asp355 residues of 2KFN. Moreover, designed drugs demonstrated improved pharmacokinetic properties. This study disclosed that 9-octadecenoic acid and drugs containing trifluoroacetyl and trifluoromethyl groups are the best 2KFN inhibitors. Overall, these results can be useful

**Electronic supplementary material** The online version of this article (doi:10.1007/s12539-016-0186-3) contains supplementary material, which is available to authorized users.

✉ Mohammad A. Halim
mahalim@grc-bd.org

Jakaria Shawon
sjakaria@grc-bd.org

Akib Mahmud Khan
amkhan@grc-bd.org

Adhip Rahman
arahman@grc-bd.org

Mohammad Mazharol Hoque
mmhoque@grc-bd.org

Mohammad Abdul Kader Khan
khanm@ucj.edu.sa

Mohammed G. Sarwar
md.sarwar@rub.de

[1] Division of Computer-Aided Drug Design, BICCB, Green Research Centre, 38 Green Road West, Dhaka 1205, Bangladesh

[2] Department of Biochemistry and Molecular Biology, University of Dhaka, Dhaka 1000, Bangladesh

[3] Department of General Studies, Jubail University College, Jubail Industrial City 31961, Saudi Arabia

[4] Fakultät für Chemie und Biochemie, Organische Chemie I, Ruhr-Universität Bochum, Universitätsstrasse 150, 44801 Bochum, Germany

[5] Present Address: Institut Lumière Matière, Université Lyon 1 – CNRS, Université de Lyon, 69622 Villeurbanne Cedex, France

Published online: 01 October 2016

for the design of new potential candidates against DNA polymerase I.

**Keywords** Rational drug design · Azelaic acid · Acne · DNA polymerase I · Density functional theory · Nonbonding interactions · Molecular docking

**Abbreviations**

| | |
|---|---|
| AzA | Azelaic acid |
| DFT | Density functional theory |
| ADMET | Absorption, distribution, metabolism, excretion, toxicity |
| QM | Quantum mechanics |
| CASTp | Computed Atlas of Surface Topography of proteins |
| SDF | Structure Data File |
| SMILES | Simplified molecular-input line-entry system |
| HOMO | Highest occupied molecular orbital |
| LUMO | Lowest unoccupied molecular orbital |
| hERG | Human ether-a-go-go-related gene |
| BBB | Blood brain barrier |

## 1 Introduction

Comprehension of molecular recognition has crucial importance in applications like chemical catalysis, therapeutics and sensor design [1]. In biological systems, molecular recognition plays a significant role in receptor-ligand complexes [2]. The selective binding capability of a molecular receptor to a ligand with high affinity involves molecular recognition by means of non-covalent bonds such as hydrogen bonds, ionic bonds and van der Waals attractions along with hydrophobic interactions [3, 4]. Identification and quantification of these weak non-covalent interactions are significant for structure-based ligand design in medicinal chemistry [5]. Particularly, hydrogen bond is an omnipresent component of molecular recognition and binding energy is at the heart of all molecular recognition and enzyme catalysis [6]. Hydrogen bonding phenomenon has been recognized in physics, chemistry and biology because of its significance [7, 8]. Both experimentally and theoretically, the physical and chemical characteristics of hydrogen bond have been widely studied due to its wide medical and engineering applications [9]. There has been particular recent interest in the intra- and inter-molecular hydrogen bonds in the excited state [10]. Molecular recognition has important role on both molecular level and macroscopic level. Macroscopic-scale recognition by means of molecular recognition shows positivity in the advancement of medical applications [11]. In the field molecular and supramolecular chemistry, intermolecular hydrogen bonding plays an important role and has crucial effects in solute–solvent interaction [12]. Addition of fluorine, trifluoromethyl or trifluoroacetyl groups in therapeutic agents influence conformation, cell membrane penetration and pharmacokinetic properties; moreover, such modification enhances metabolic durability of the compounds and formation of more non-covalent interactions—thereby increasing the binding affinity [13–18].

DNA polymerases are key enzymes in DNA molecule synthesis from deoxyribonucleotides, the building blocks of DNA. The primary role of DNA polymerases is to replicate the genome accurately to ensure the conservation of genetic information from generation to generation [19]. DNA polymerase has to form hydrogen bonds for base pairing from an existing single template strand and free nucleotides in solution, and to do so with high specificity for forming correct pairs rather than incorrect ones [20, 21]. Replicative DNA polymerases are essential in all living organisms for DNA synthesis using the genomes [22]. It participates in the process of DNA replication which is the first evidence of the existence of an enzymatic activity capable of synthesizing DNA [23]. *E. coli* Pol I was the first DNA polymerase to be isolated and the first polymerase whose structure was solved [24]. Bacterial DNA polymerase I is involved in bacterial DNA synthesis and lesion repair [25]. In this study, we used the Klenow fragment of DNA Pol I (*E. coli*) crystal structure which is a cleaved product of protease subtilisin [26]. Mentioned Klenow fragment has DNA polymerase and 3′–5′ editing exonuclease enzymatic activity, which are located on separate structural domains of the molecule [27]. Amino acid sequence homology showed that the 3′ → 5′ exonuclease active site of *E. coli* DNA polymerase I is conserved for both prokaryotic and eukaryotic DNA polymerases [28].

Acne is one of the most common follicular, sometime chronic inflammatory diseases of skin mostly occurring in younger people. It virtually happens to everyone and can be characterized by many features such as pimples, abscess, blackhead, cysts and in some cases scarring [29–32]. In the time of adolescence, it occurs due to the excess production of androgenic hormones such as testosterone. Other reasons such as hyper-proliferation of keratinocytes, inflammation and bacterial colonization in the hair follicles can also lead to the formation of acne [33, 34]. It is the most common skin disorder in USA costing over 3 billion dollars per year in the terms of treatment of acne and loss of productivity [29, 35].

Azelaic acid [AzA, formula $(CH_2)_7(CO_2H)_2$] is a naturally occurring saturated dicarboxylic acid. It is used as a topical cream to treat mildly to moderately inflamed acne [36, 37]. It has many proposed mechanisms of action such as antimicrobial, anti-inflammatory, antioxidant and

keratinolytic reaction. It is also non-toxic, non-teratogenic and non-mutagenic [38, 39]. AzA is reported to have potent inhibitory effect on replication of DNA because it interferes with activities of enzymes such as DNA polymerases which are required for DNA synthesis. In keratinocytes, AzA can hinder cell proliferation by competitively inhibiting DNA synthesis [28, 29]. In some studies, it was found that AzA is used in dose- and time-dependent manner to exert its anti-proliferative cytostatic effects on keratinocytes [29–31]. Moreover, AzA can also prevent growth and proliferation of abnormal melanocytes by inhibiting DNA synthesis along with other mechanisms [32]. On topical application, azelaic acid (20 %) is effective in rosacea, comedonal acne and inflammatory acne treatment [36, 40]. Microbial cellular protein synthesis can be inhibited by the azelaic acid's antimicrobial action that may help to stop the proliferation of acne causing bacteria such as *Propionibacterium acnes* and *Staphylococcus epidermidis* [36, 41]. It was successfully used in the clinical treatment of seven cases of lentigo maligna in that remission of the lesions was observed [42]. Protein synthesis is significantly more sensitive to the action of AzA than both RNA and DNA synthesis [43].

In this study, we employ density functional theory to optimize azelaic acid and its related compounds. Thermodynamic properties and frontier molecular orbitals of those drugs are also explored in details. Molecular docking calculation has been performed to understand the nonbonding interaction between designed drugs with DNA polymerase I (2KFN). Some of these drugs show a better binding affinity and nonbonding interaction with the target molecule in comparison with azelaic acid.

## 2 Methodology and Computational Details

### 2.1 Optimization of Ligands Using Quantum Mechanical Calculations

Quantum mechanical (QM) methods allow us to calculate internal energies precisely and interpret various types of complicated interactions between ligands and target proteins such as hydrogen bonds, hydrophobic interactions and electrostatic interactions [44]. The QM calculation was simulated using density functional theory employing Becke's (B) [45] exchange functional combining Lee, Yang and Parr's (LYP) correlation functional [46] in Gaussian 09 program package for all drugs [47]. Pople's 6-31G(d,p) basis set was used for all calculations. Initial geometry of azelaic acid was taken from the crystal structure [48]. The optimized structure of azelaic acid was manipulated replacing hydrogen with $-CF_3$, $-COF_3$, F, glycine, hydrazide and methoxy groups. These modified compounds, labeled from A1 to A8 sequentially presented in Fig. 1, were then optimized using the same level of theory. For each of the molecules, internal electronic energy, enthalpy, free energy and dipole moment were explored.

Same level of theory was used to do the molecular orbital calculations. Hardness ($\eta$) and softness ($S$) of all drugs were also calculated from the energies of frontier HOMOs and LUMOs considering Parr and Pearson interpretation [49, 50] of harness in DFT and Koopmans theorem [51] on the correlation of ionization potential ($I$) and electron affinities ($E$) with HOMO and LUMO energy ($\varepsilon$). The following equations are used for Hardness ($\eta$) and softness ($S$):

$$\eta = [\varepsilon\mathrm{LUMO} - \varepsilon\mathrm{HOMO}]/2$$

$$S = 1/\eta$$

### 2.2 Preparation of Target Protein Structure for Docking

The modified drugs were subjected to molecular docking study with DNA polymerase I (2KFN). Crystal structure was collected from the Protein Data Bank (PDB) database (PDB ID: 2KFN) [52]. The crystal structure was checked followed by energy minimization done with Swiss-Pdb Viewer software packages (version 4.1.0), whereas the crystal structure has some issues related to improper bond order, side chains geometry and missing hydrogen(s) [53]. The highest binding pocket area and volume of active binding site of the protein structure was calculated using CASTp [54]. The highest pocket area and volume of optimized protein structure was found to be 1975.7 $\text{Å}^2$ and 5492.6 $\text{Å}^3$, respectively. CASTp calculations also provided the amino acid residues present in the active site along with their residue number (Figure S1). PyMol (version 1.3) software packages were used to erase all the hetero atoms and water molecules before docking [55]. Finally, we saved both the proteins and ligand structures in .PDBQT format as it is the only one supported file format that required by Autodock Vina (Vina) software (version 1.1.2, May 11, 2011) for docking analysis [56].

### 2.3 Analysis and Visualization of Docking Results

Molecular docking is an important tool in computational drug design which can predict the predominant binding mode(s) of a ligand with the target protein [57]. To dock the compounds against 2KFN, the center grid box was set at 58.204, 12.252 and 96.186 Å and box size was set at 61.970, 87.051 and 73.760 Å in $x$, $y$ and $z$ direction, respectively. In the current work, rigid docking was performed using Autodock Vina [58]. During rigid docking

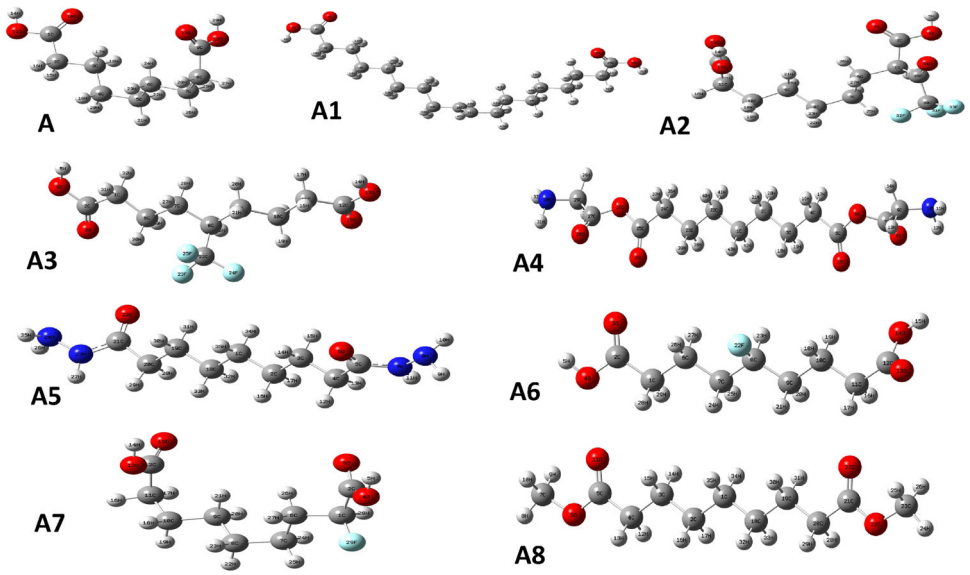


**Fig. 1** Optimized structure of Azelaic acid(A) and its modified derivatives (A1,A2,A3,A4,A5,A6,A7 and A8)

for all the ligands, all rotatable bonds are converted into non-rotatable and then binding affinities are predicted by using Autodock Vina docking protocol. A detailed analysis of residues involved in the interaction between ligands and target protein was conducted to visualize and interpret the hydrogen bond interactions, hydrophobic interactions of the best poses of drugs with the respective protein using the Accelrys Discovery Studio 4.1 [59], and LigPlot+ version v1.4.5 [60].

### 2.4 Pharmacokinetic Parameters

AdmetSAR online database has been utilized to predict the data related to drug absorption, metabolism and carcinogenicity for azelaic acid and its modified derivatives [61]. Structure Data File (SDF) and simplified molecular-input line-entry system (SMILES) strings were utilized throughout the generation process.

## 3 Results and Discussion

The image of frontier molecular orbitals of **A** and **A1** is displayed in Fig. 2. Interactions of **A**, **A1**, **A2** and **A3** with 2KFN are presented in Fig. 3. Figure 4 illustrates a more precise view of the interactions, including the hydrophobic binding sites of **A**, **A1** and **A2**. Hydrogen bond surface of 2KFN with **A**, **A1**, **A2** and **A3** is shown in Fig. 5. The stoichiometry, electronic energy, enthalpy, free energy and dipole moment of all drugs are reported in Table 1. The HOMO and LUMO energies, gap, hardness and softness of all drugs are presented in Table 2. The binding affinity and all nonbonding interaction of all drug-receptors complexes are summarized in Table 3. Partial charges of **A**, **A1**, **A2** and **A3** are illustrated in the supplementary Figure S2, and graphs for atomic charges of **A**, **A1**, **A2** and **A3** are given in Fig. 6 and Figure S3.

### 3.1 The Electronic Structure of Azelaic Acid (A) and it's Modified Derivatives

Modifications of azelaic acid with trifluoroacetyl group, trifluoromethyl group, glycine and hydrazide significantly influence the structural properties including energy, partial charge distribution and dipole moment. After introduction of these groups, more negative values are observed for the energy, enthalpy and free energies. These results demonstrate that after modification, structures become more stable than the parent structure (Table 1). Free energy is a pivotal criterion to represent the interaction of binding partners where both the sign and magnitude are important to express the likelihood of biomolecular events occurring. Positive free energy values indicate that energy is required to drive the interaction and binding will not occur spontaneously [62]. All the values in this inquiry are negative (Table 1) meaning the binding will occur spontaneously without any extra energy expenditure. Appreciable changes are observed for **A1**, **A2**, **A3** and **A4**, hence suggesting 9-Octadecenoic acid, trifluoroacetylated and trifluoromethylated molecules are energetically and configurationally more preferable. The highest free energy change is observed for **A2**. Here, one hydrogen atom is replaced with trifluoroacetyl group at the position C-1 which changes the free energy of the structure from −653.356 Hartree to −1103.687 Hartree. However, in case of **A5**, **A6**, **A7** and **A8**, these values are marginally changed.

The calculated dipole moments of these drugs have also changed. Elevated level of dipole moment enhances the

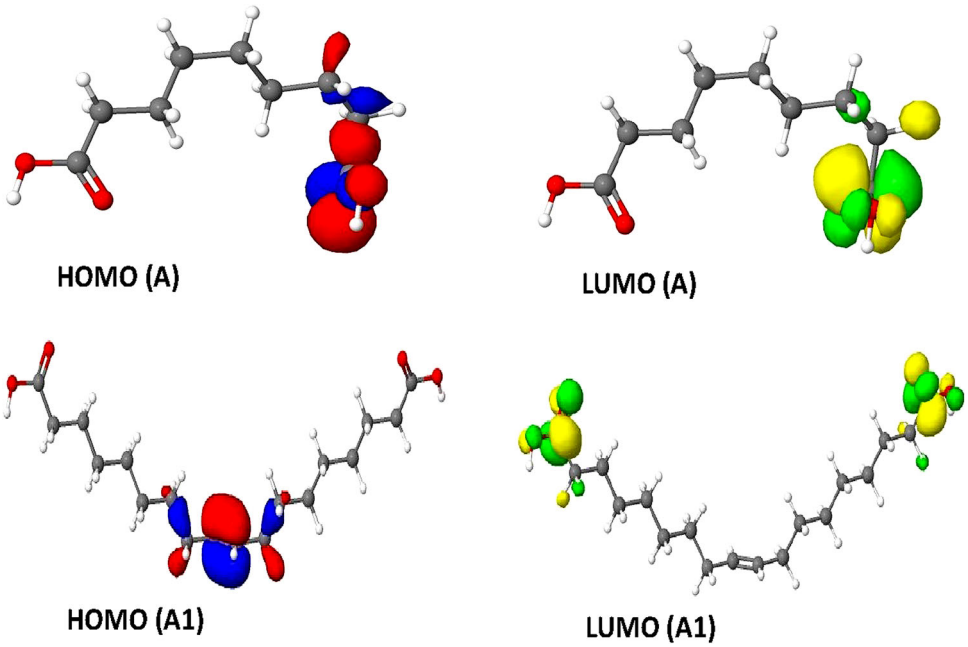


**Fig. 2** Frontier molecular orbitals (HOMO and LUMO) of A and A1

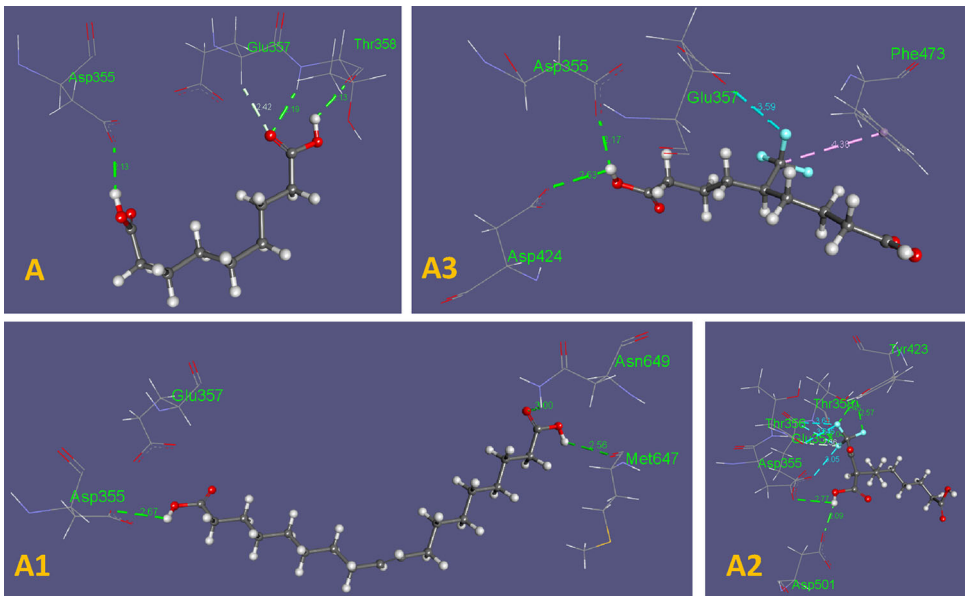


**Fig. 3** Nonbonding interactions of A, A1, A2 and A3 with 2KFN generated by Discovery Studio

polar nature of a molecule [63]. The dipole moment of AzA is found to be 2.363 Debye, and here all modified drugs except **A2** and **A7** show increased dipole moment (Table 1). Large increase is observed in **A1** (7.244 Debye) and **A3** (7.810 Debye). Elevated dipole moment can promote hydrogen bond and nonbonded interactions in drug-receptor complexes which in turn can lead to increased binding affinity [64–66]. Therefore, for **A1** and **A3**, increased dipole moment resulted in increased binding affinity against 2KFN.

Polarity of chemical bonds often dictates the structure and reactivity [67]. The dipole moment is just a vector, but it does not give the polarity of the molecule. A number of different methods have been proposed for assigning partial charges to the atoms of a molecule, including both quantum chemical and empirical schemes [68]. Three different methods (Mulliken, NBO and Hirshfeld) are used here to compute the atomic partial charges of our parent compound **A** and modified compounds **A1**, **A2**, **A3**. In **A**, C-1 and C-9 atoms show positive charge when calculated with Mulliken and NBO methods, however, show slightly negative value with Hirshfeld method (Fig. 6). Similarly, 12-O and 13-O atoms exhibit negative charge with Mulliken and NBO

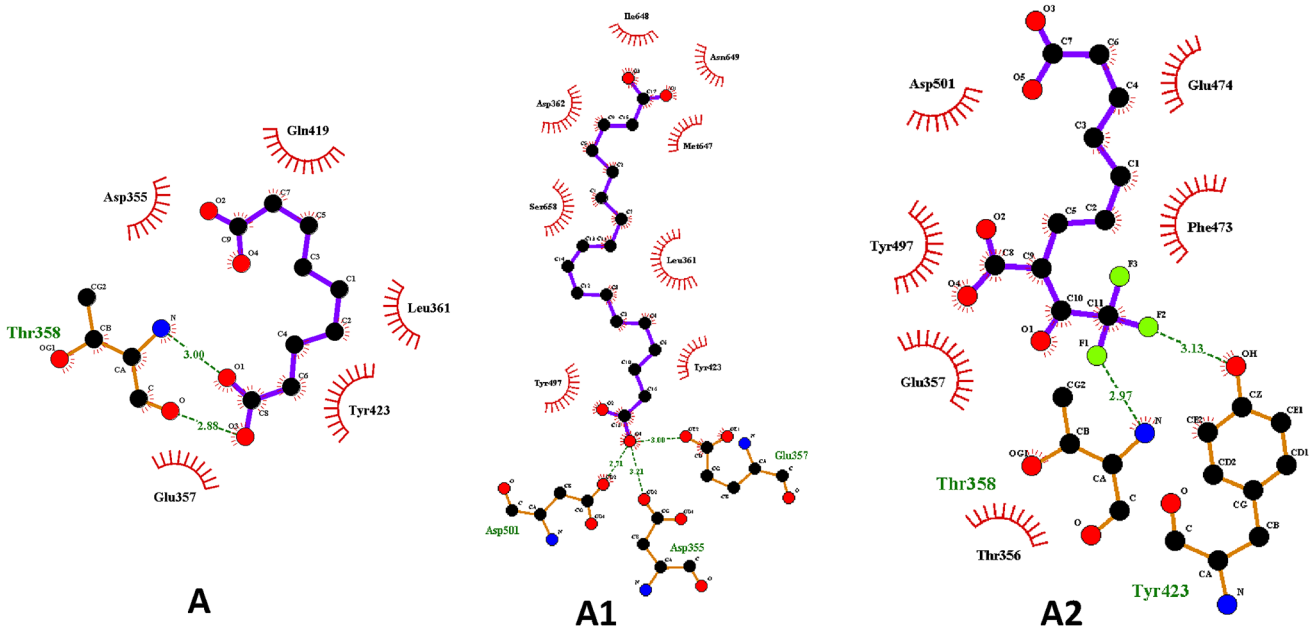


**Fig. 4** Nonbonding and hydrophobic binding sites of A, A1 and A2 with 2KFN generated by LigPlot+

**Table 1** Stoichiometry, electronic energy, enthalpy, Gibbs free energy in Hartree and dipole moment (Debye) of Azelaic acid and its derivatives

| Name | Stoichiometry | Electronic energy | Enthalpy (Hartree) | Gibbs free energy (Hartree) | Dipole moment (Debye) |
|---|---|---|---|---|---|
| **A** | $C_9H_{16}O_4$ | −653.295 | −653.294 | −653.356 | 2.363 |
| **A1** | $C_{18}H_{32}O_4$ | −1005.651 | −1005.650 | −1005.742 | 7.244 |
| **A2** | $C_{11}H_{15}F_3O_5$ | −1103.612 | −1103.611 | −1103.687 | 2.285 |
| **A3** | $C_{10}H_{15}F_3O_4$ | −990.305 | −990.304 | −990.375 | 7.810 |
| **A4** | $C_{13}H_{22}N_2O_6$ | −1069.157 | −1069.156 | −1069.244 | 3.471 |
| **A5** | $C_9H_{20}N_4O_2$ | −724.119 | −724.118 | −724.189 | 6.406 |
| **A6** | $C_9H_{15}FO_4$ | −752.536 | −752.535 | −752.599 | 3.210 |
| **A7** | $C_9H_{15}FO_4$ | −752.526 | −752.524 | −752.590 | 1.870 |
| **A8** | $C_{11}H_{20}O_4$ | −731.849 | −731.848 | −731.920 | 3.001 |

**Table 2** Energy (atomic unit) of HOMOs, LUMO, Gap, Hardness and Softness of all drugs

| Molecules | εHOMO-1 (Hartree) | εHOMO (Hartree) | εLUMO (Hartree) | Gap (Hartree) | $\eta$ (hardness) | $S$ (softness) |
|---|---|---|---|---|---|---|
| **A** | −0.2745 | −0.2691 | 0.0108 | 0.2799 | 0.1399 | 7.148 |
| **A1** | −0.2701 | −0.2382 | 0.0123 | 0.2505 | 0.1253 | 7.981 |
| **A2** | −0.2869 | −0.2717 | −0.0661 | 0.2056 | 0.1028 | 9.728 |
| **A3** | −0.2766 | −0.2756 | 0.0059 | 0.2815 | 0.1408 | 7.105 |
| **A4** | −0.2445 | −0.2445 | −0.0297 | 0.2149 | 0.1074 | 9.311 |
| **A5** | −0.2359 | −0.2350 | 0.0394 | 0.2745 | 0.1372 | 7.289 |
| **A6** | −0.2773 | −0.2713 | 0.0078 | 0.2792 | 0.1396 | 7.166 |
| **A7** | −0.2815 | −0.2715 | −0.0018 | 0.2697 | 0.1349 | 7.416 |
| **A8** | −0.2690 | −0.2685 | 0.0162 | 0.2847 | 0.1424 | 7.025 |

methods, but positive values are observed in case of Hirshfeld method. In **A1**, **A2** and **A3**, however, all atoms show consistent sign of charge when calculated with different methods. In **A**, **A1**, **A2** and **A3**, charges of the electronegative atoms (such as O, F) tend to be much more negative when calculated with NBO method than the corresponding charges when calculated with Mulliken or Hirshfeld method (Fig. 6 and Figure S3).

**Table 3** Binding energy and nonbonding interaction of Azelaic acid and its modified derivatives after rigid docking

| Compund | Docking against DNA polymerase I(2KFN) | | | | | | | | |
|---|---|---|---|---|---|---|---|---|---|
| | Binding energy (kcal/mol) | H-bond | | Halogen bond | | Hydrophobic interaction | | Electrostatic interaction | |
| | | (Amino acid… **Ligand atom**) | Distance (Å) | (Amino acid… **Ligand atom**) | Distance (Å) | (Amino acid… **Ligand atom**) | Distance (Å) | (Amino acid… **Ligand atom**) | Distance (Å) |
| **A** | −6.7 | Thr358[N–H…**O**] | 2.19 | – | – | – | – | – | – |
| | | Thr358[O…**H–O**] | 2.13 | | | | | | |
| | | Glu357[C–H…**O**] | 2.42 | | | | | | |
| | | Asp355[O…**H–O**] | 2.13 | | | | | | |
| **A1** | −8.7 | Asp355[O…**H–O**] | 2.67 | – | – | – | – | – | – |
| | | Met647[O…**H–O**] | 2.56 | | | | | | |
| | | Asn649[N–H…**O**] | 3.00 | | | | | | |
| **A2** | −8.6 | Thr358[N–H…**F**] | 2.04 | Glu357[C…**F**] | 3.64 | – | – | – | – |
| | | Asp355[O…**H–O**] | 2.77 | Glu357[C…**F**] | 3.64 | | | | |
| | | Tyr423 [O–H…**F**] | 2.57 | Glu357[O…**F**] | 3.05 | | | | |
| | | Tyr423[O–H…**F**] | 2.45 | Thr356[O…**F**] | 3.15 | | | | |
| | | Asp501[O…**H–O**] | 2.09 | | | | | | |
| **A3** | −7.9 | Asp355[O…**H–O**] | 2.17 | Glu357[O…**F**] | 3.59 | Phe473[Alkyl…Pi] | 4.38 | – | – |
| | | Asp424[O…**H–O**] | 2.53 | | | | | | |
| **A4** | −7.8 | Thr358[N–H…**O**] | 2.94 | – | – | – | – | – | – |
| | | Glu357[C–H…**O**] | 3.61 | | | | | | |
| | | Asp355[O…**H–N**] | 2.74 | | | | | | |
| | | Thr356[O…**H–N**] | 2.15 | | | | | | |
| | | Tyr423[O–H…**O**] | 2.63 | | | | | | |
| | | Lys481[O…**H–C**] | 2.67 | | | | | | |
| **A5** | −7.7 | Gln419[O…**H–N**] | 1.89 | – | – | – | – | Asp424[O…**H–N**] | 2.32 |
| | | Gln483[O…**H–N**] | 2.87 | | | | | Asp424[O…**H–N**] | 2.60 |
| | | Leu484[O…**H–N**] | 2.66 | | | | | Asp424[O…**H–N**] | 2.99 |
| | | Thr485[C–H…**N**] | 2.62 | | | | | Asp355[O…**H–N**] | 2.32 |
| | | Phe486[N–H…**O**] | 2.77 | | | | | | |
| **A6** | −7.2 | Asp355[O…**H–O**] | 2.02 | – | – | Phe473[Alkyl…Pi] | 4.90 | – | – |
| | | Asp424[O…**H–O**] | 2.65 | | | | | | |
| | | Phe486[N–H…**O**] | 2.18 | | | | | | |
| **A7** | −6.8 | Thr358[N–H…**O**] | 1.85 | Thr358[N–H…**F**] | 2.55 | – | – | – | – |
| | | Thr358[N–H…**F**] | 2.55 | Glu357[C-H…**F**] | 2.40 | | | | |
| | | Thr358[O…**H–O**] | 2.69 | Thr356[O…**F**] | 3.18 | | | | |
| | | Glu357[C–H…**O**] | 2.82 | | | | | | |
| | | Glu357[C–H…**F**] | 2.40 | | | | | | |
| **A8** | −6.2 | Asp501[O…**H–C**] | 2.56 | – | – | Met458[Alkyl] | 4.86 | – | – |

HOMO and LUMO are acronyms for highest occupied molecular orbital and lowest unoccupied molecular orbital, respectively. Frontier molecular orbital theory tells us HOMO and LUMO play an important role in many chemical reactions [69]. The HOMO–LUMO gap is related to the chemical hardness and softness of a molecule [70, 71]. High kinetic stability and low chemical reactivity are associated with a large HOMO–LUMO gap [72]. A small HOMO–LUMO gap signifies low kinetic stability, because addition of electrons to a high-lying LUMO and/or removal of electrons from a low-lying HOMO is energetically favorable in any potential reaction [72–74]. HOMO–LUMO gap as well as hardness and softness was calculated for the modified drugs (Table 2). In this analysis, we found that drug with trifluoroacetyl group (**A2**) has the lowest HOMO–LUMO gap and the highest softness, which may

contribute to its higher chemical activity than AzA and other modified drugs. A decreased HOMO–LUMO gap in most of the modified drugs promotes softness which makes them relatively more polarizable and chemically more reactive compared to AzA. However, in **A8**, addition of methoxy group increased the energy gap significantly, thus lowering the chemical reactivity.

### 3.2 Interaction and Binding Affinity of Azelaic Acid (A) and Modified Azelaic acid (A1, A2 and A3) with 2KFN

We use 9-Octadecenoic acid as **A1**. The first pose of **A1**, **A2** and **A3** agreed most with the first pose of **A**, so values associated with these poses were chosen for studying interaction and binding affinity. **A** is the parent drug azelaic acid (AzA), and **A2** is one of the modified drugs where trifluoroacetyl group was added to position 2C of AzA. Trifluoroacetyl group is already being integrated in many inhibitors of enzymes as a key functional group which has shown exceptionally high potency [75–77]. Addition of trifluoroacetyl to AzA caused significant changes to energy, partial charge distribution and dipole moment. We found improved electronic energy, enthalpy and free energy for **A1**, **A2** and **A3** compared to **A**. In modified drug **A3**, trifluoromethyl (–CF3) group has been incorporated into the middle (5C) of the AzA. CF3 group has great significant application in agrochemical dyes and pigments, pharmaceuticals, polymers and material chemistry when CF3 incorporated to different organic molecules [78–80]. Strong electronegativity and hydrophobic nature are two critical characteristics of trifluoromethyl group which can be used in drug design to develop selective functionality which are connected to physiochemical, biological and pharmacological properties [81]. In some modified molecules, halogen bonds, absent in AzA, are observed due to the presence of halogen molecule(s). Some recent studies showed halogen bonding similar to hydrogen bonding plays a crucial role in both biological and chemical system [82–87]. In our study, **A2**, **A3** and **A7** show several halogen bonds (Fig. 3).

The binding affinities of **A1**, **A2** and **A3** with 2KFN have considerably increased to −8.7, −8.6 and −7.9 kcal/mol, respectively, from −6.7 kcal/mol of **A**. Improved hydrogen bonding observed in **A2** not only contribute in increasing binding affinity but can also enhance binding specificity [88, 89]. In biology, hydrogen bonding is essential for DNA structure. Depending on the nucleotide sequence, a regular helical structure of the DNA helix is dictated by specific hydrogen bonding patterns [90]. In the **A2**-2KFN docked structure, multiple nonbonded interactions were observed. In a literature, it is suggested hydrogen bond of <2.3 Å can increase binding affinity by several magnitude [91]. A strong fluorine hydrogen bond with Thr358 (2.04 Å) and a strong hydrogen bond with Asp501 (2.09 Å) are observed in **A2**-2KFN complex. Thus, strong hydrogen bonding is the most significant contributing factor in increasing binding affinity of **A2** with 2KFN. Non-covalent interactions such as hydrogen bond, halogen bond and hydrophobic interaction are involved in the binding of modified drug **A3** with 2KFN (Fig. 3). The **A3**-2KFN complex is stabilized by two hydrogen bonds, one hydrophobic interaction and one halogen bond (Table 3). A strong hydrogen bond with Asp355 (2.17 Å) is present. Moreover, fluorine bond interactions with Glu357 are observed in case of both **A2** and **A3**. Hydrogen bond interactions with residue Asp355 are observed in **A** and all other derivatives of **A** except for **A5**, **A7** and **A8**. The structures and reactivity of many molecular systems can be determined by intermolecular hydrogen bonding [92, 93]. Among various factors, hydrogen bonding is the one which can affect selectivity of nucleotide incorporation by a DNA polymerase [94]. For drug binding, hydrogen bonds have important function in determining the accuracy of ligand binding [91]. The most notable fact here is that the F atoms of the –COCF3 group in **A2**-2KFN complex interacted with amino acids to form strong halogen bond interactions. We observed four fluorine bonds (halogen bond) in **A2**-2KFN complex and one in **A3**-2KFN complex (Fig. 3) which may have positive effect on the protein–ligand stability, as well as in the binding affinity and selectivity. In one study, it was reported that stability of protein–ligand may be increased due to the establishment of a halogen bond and thus contributes to the binding affinity and selectivity [20]. **A2** has the highest softness among the modified drugs which may promote the polarizable nature of the drug that can simulate greater nonbonding interactions with the receptor [21]. Hydrogen bond surface shows residues such as Asp355, Met647, Glu357, Asp501, Asp424, Thr356 help in creating strong acceptor regions and residues such as Thr358, Asn649, Tyr423 help in creating strong donor regions on the drug-protein interaction surface (Fig. 5). Nonbonding contacts surrounding azelaic acid and its modified forms (**A1**, **A2** and **A3**) in 2KFN are involved the following amino acid residues Glu357, Asp355, Asp 501, Thr358, Asp424, Tyr423, Thr356, Met647, Asn649 (Fig. 3). Derbyshire et al. reported to have observed interactions with Glu357, Asp355, Asp 501, Thr358, Asp424, Tyr423 while using deoxycytidine monophosphate (dCMP) or deoxythymidine monophosphate (dTMP) as substrate or inhibitor in their studies [27, 95]. In our study, we also observed such interactions while using AzA and other modified compounds. This observation helped to confirm that AzA and its derivatives are binding at the desired binding site of DNA polymerase after molecular docking.

Phe473 was found to donate its π-electrons cloud toward the alkyl chain and the carbon attached to F of the drug, thus

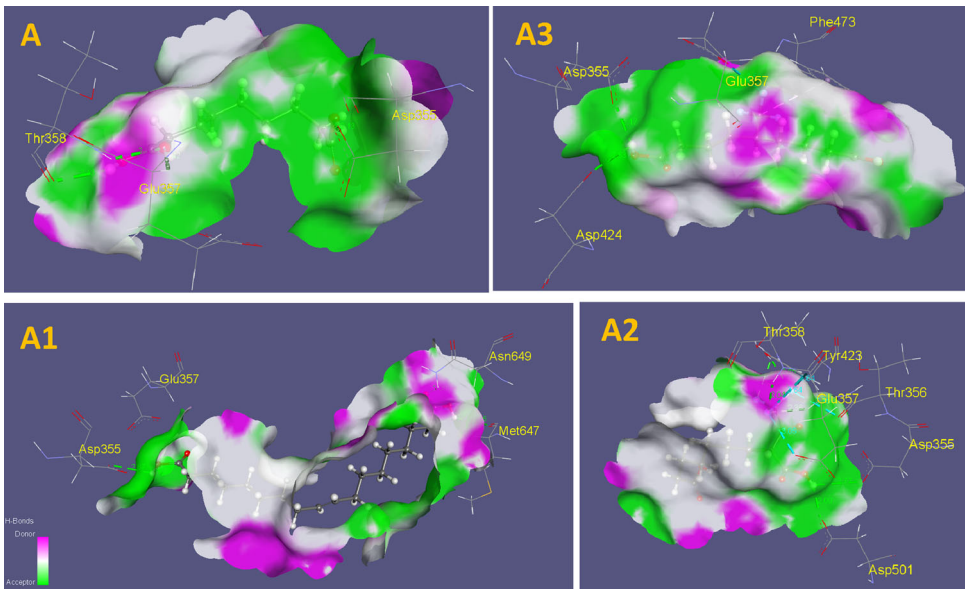


**Fig. 5** Hydrogen bond surface of 2KFN with A, A1, A2 and A3

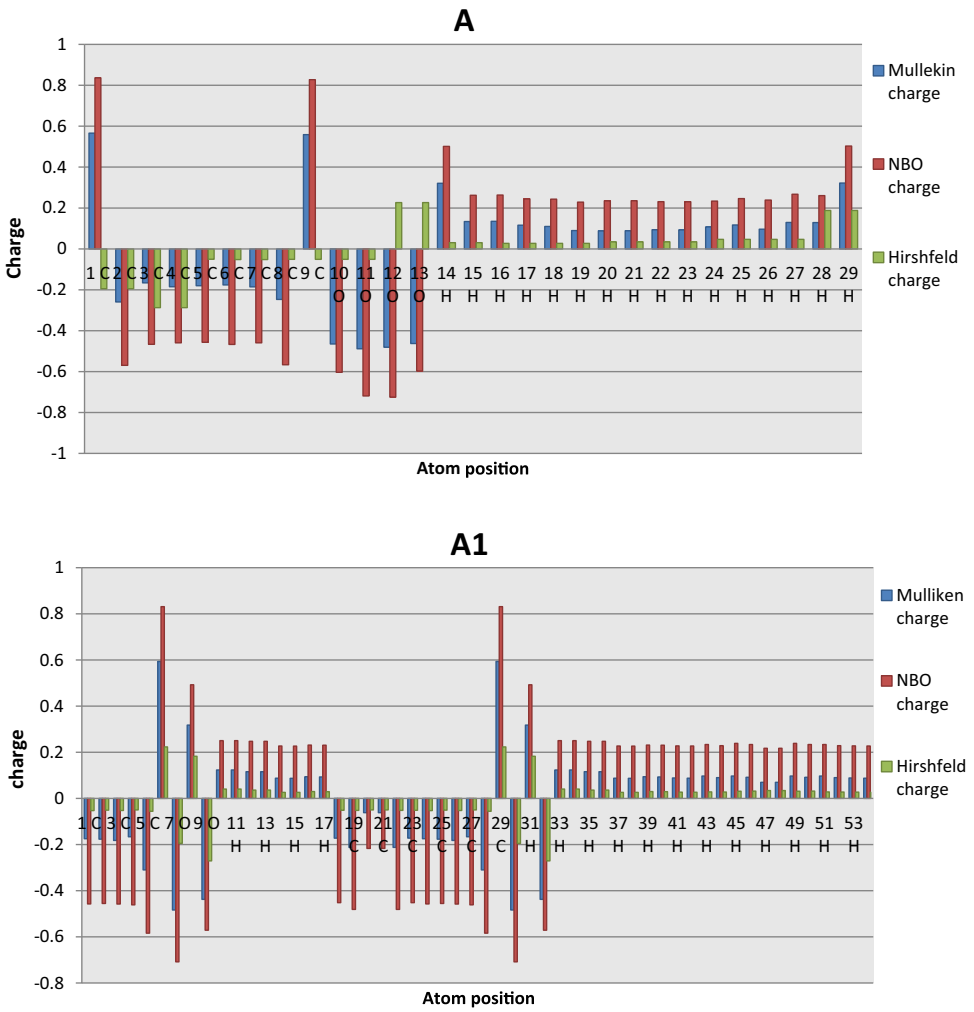


**Fig. 6** Graphs of atomic Charges of A and A1 calculated with Mulliken, NBO and Hirshfeld methods

forming few π-stacking interactions. A distinct alkyl-pi interaction (4.38 Å) with Phe473 is also observed in **A3** (Fig. 3). Neighboring aromatic rings in protein–ligand complexes from diverse families can preferably form X…π interactions with organic halogens. Clearly, these interactions can be exploited in structure-based drug design [20]. Aromatic surface shows residues such as, Tyr423, Phe473 help to create strong face region in drug-protein interaction surface of 2KFN, whereas Glu357, Thr358, Asp355 and Asp501 helps to create strong edge region during interaction surface.

### 3.3 Interaction and Binding Affinity of Azelaic Acid (A) and Modified Azelaic Acid (A4, A5 A6, A7 and A8) with 2KFN

Glycine, hydrazide and methoxy groups are used as functional group in **A4**, **A5** and **A8**, respectively. In case of **A6** and **A7**, fluorine is used as functional group for modification. The third pose of **A4** is chosen as it agreed most with the first pose of A, so values associated with this pose were chosen for studying interaction and binding affinity. The binding affinities of **A4**, **A5** and **A6** with 2KFN are −7.8, −7.7 and −7.2 kcal/mol, respectively. Hydrogen bonding has considerably increased in both **A4** and **A5**. A strong hydrogen bond with Thr356 (2.15 Å) is observed in **A4** along with two non-conventional hydrogen bonds Glu357 (3.61 Å) and Lys481 (2.67 Å) which could be the major contributing factor for improved binding of **A4** with 2KFN. Basically, the CH…O bonding termed as non-conventional hydrogen bond, slightly weaker than its classical OH…O hydrogen bond, is believed to be critical in a large number of biomacromolecules' crystal structures [96, 97]. Several electrostatic interactions are observed for **A5** with Asp424 and Asp355. A strong hydrogen bond with Gln419 (1.89 Å), absent in **A**-2KFN complex, is found in **A5**-2KFN complex along with several other hydrogen bonds. These interactions could be the key factors for the improved binding of **A5** with 2KFN. In **A6**, an alkyl-pi interaction with Phe473 (4.90 Å) and three hydrogen bonds are present. Binding affinity of **A7** against 2KFN (−6.8 kcal/mol) has not increased compared to **A**, while in **A8** binding affinity has decreased to −6.2 kcal/mol. We noticed only one hydrogen bond and one alkyl interaction in **A8**. Hydrogen bond interactions have significantly decreased in **A8** which could be liable for its weaker binding affinity with 2KFN.

### 3.4 Pharmacokinetic Properties of Azelaic Acid and its Modified Derivatives

AdmetSAR calculation predicts all drugs are non-carcinogenic. So, the modified drugs are expected to be safe for topical use. All drugs are P-glycoprotein non-inhibitor, and modified drugs containing glycine and hydrazide show lower probability values. P-glycoprotein inhibition can block the absorption, permeability and retention of the drugs [98]. The drugs show positive response for blood brain barrier (BBB) criteria, predicting that drugs will go through BBB. However, azelaic acid and the modified derivatives show weak inhibitory property for human ether-a-go-go-related gene (hERG). Inhibition of hERG can lead to long QT syndrome [99], so more study on this aspect is necessary. We also calculated the inhibition constant of all the drugs using $E + I \leftrightarrow EI$, where E is the enzyme and I is the inhibitor molecule (the reference concentrations for all the entities have been considered 1 mol $L^{-1}$ for the calculations) and the relationship

$$\ln K_b = -\ln K_i,$$

where $\ln K_b = -\Delta G/RT$, $\Delta G$ = free energy of binding and are presented in the last row of Table 4.

**Table 4** Selected pharmacokinetic parameters of Azelaic acid and its derivatives (Probability values related to each of the parameters are given in the parenthesis)

| Parameters | A | A1 | A2 | A3 | A4 | A5 | A6 | A7 | A8 |
|---|---|---|---|---|---|---|---|---|---|
| Blood brain barrier | + (0.7397) | + (0.7666) | + (0.9526) | + (0.9302) | + (0.8104) | + (0.9934) | + (0.8814) | + (0.8814) | + (0.9654) |
| Human intestinal absorption | + (0.5731) | + (0.7351) | + (0.8890) | + (0.8324) | + (0.6900) | + (0.9390) | + (0.7779) | + (0.7779) | + (0.7681) |
| P-glycoprotein inhibitor | NI (0.9845) | NI (0.9809) | NI (0.9600) | NI (0.9688) | NI (0.8804) | NI (0.8279) | NI (0.9709) | NI (0.9709) | NI (0.8864) |
| Human ether-a-go-go-related (hERG) gene inhibition | WI (0.9348) | WI (0.9166) | WI (0.9580) | WI (0.9693) | WI (0.8568) | WI (0.9230) | WI (0.9701) | WI (0.9701) | WI (0.9101) |
| Carcinogen | NC (0.8382) | NC (0.8374) | NC (0.7775) | NC (0.7949) | NC (0.6920) | NC (0.5574) | NC (0.7970) | NC (0.7970) | NC (0.6738) |
| Ki (at 298 K), nM | 12,396.4 | 425.2 | 503.3 | 1638.6 | 1939.6 | 2295.9 | 5334.9 | 10,472.8 | 28,805.1 |

*NI* Non-inhibitor, *WI* weak inhibitor, *NC* non-carcinogen

Lower $K_i$ values of the A1 (9-octadecenoic acid) and A2 (trifluoroacetylated) are reflective of their improved binding affinity against 2KFN.

## 4 Conclusion

In this study, we have shown the relation and binding interactions between the designed drugs and 2KFN. Some interesting features are revealed related to charge distribution, dipole moment, enthalpy, free energy and molecular orbitals with the help of density functional theory calculation. Enhanced free energy and enthalpy make the modified drugs thermodynamically more stable. Moreover, HOMO–LUMO gap of modified drugs is reasonably lower than azelaic acid, except for **A3** and **A8**, indicating that those compounds are chemically more reactive. The strong binding affinity is found for **A1**-2KFN complex, and we found that our best modified drug has low kinetic stability and high chemical reactivity. Enhanced hydrogen bonding between the modified drugs and 2KFN has important contribution in higher binding affinity. Pi-alkyl interaction is found in **A3**-2KFN complex, and fluorine bonds are observed for modified compounds **A2**, **A3** and **A7** with 2KFN. In our study, we observed that Asp355 is an important residue in drug-protein interaction as this residue interacts with azelaic acid and most of its modified forms (**A1**, **A2**, **A3**, **A4**, **A5**, **A6**). Pharmacokinetic calculation predicts all drugs are non-carcinogenic. Therefore, modified compounds **A1**, **A2**, **A3**, and **A4** can be potential candidates for better performance.

**Acknowledgments** We are grateful to our donors who supported to build a computational platform in Bangladesh http://grc-bd.org/donate/.

**Author's Contribution** MAH, MGS and MAKK conceived the idea. MAH, MGS, MAKK and MMH designed the drugs. JS performed the quantum calculations. JS, AMK and AR performed the molecular docking, ADME calculations, data collection and draft writing. All authors read and approved the manuscript.

**Funding** This research does not receive any external funding.

**Compliance with ethical standards**

**Conflict of interest** Authors declare that there are no competing interests regarding the publication of this paper.

## References

1. Zhang J, Landry MP, Barone PW et al (2013) Molecular recognition using corona phase complexes made of synthetic polymers adsorbed on carbon nanotubes. Nat Nanotechnol 8:959–968. doi:10.1038/nnano.2013.236
2. Breiten B, Lockett MR, Sherman W et al (2013) Water networks contribute to enthalpy/entropy compensation in protein-ligand binding. J Am Chem Soc 135:15579–15584. doi:10.1021/ja4075776
3. Lehn JM (1992) Supramolecular chemistry: from molecular recognition towards molecular information processing and self-organization. Mater Sci Forum 91–93:100. doi:10.4028/www.scientific.net/MSF.91-93.100
4. Alberts B, Johnson A, Lewis J et al (2002) Protein Function. In: Molecular Biology of the Cell, 4th edn. Garland Science, New York
5. Persch E, Dumele O, Diederich F (2015) Molecular recognition in chemical and biological systems. Angew Chemie Int Ed. doi:10.1002/anie.201408487
6. Fersht AR (1987) The hydrogen bond in molecular recognition. Trends Biochem Sci 12:301–304
7. Zhao GJ, Han KL (2007) Early time hydrogen-bonding dynamics of photoexcited coumarin 102 in hydrogen-donating solvents: theoretical study. J Phys Chem A 111:2469–2474. doi:10.1021/jp068420j
8. Zhao J, Chen J, Cui Y et al (2015) A questionable excited-state double-proton transfer mechanism for 3-hydroxyisoquinoline. Phys Chem Chem Phys 17:1142–1150. doi:10.1039/c4cp04135f
9. Zhao G-J, Han K-L (2012) Hydrogen bonding in the electronic excited state. Acc Chem Res 45:404–413. doi:10.1021/ar200135h
10. Zhao J, Chen J, Liu J, Hoffmann MR (2015) Competitive excited-state single or double proton transfer mechanisms for bis-2,5-(2-benzoxazolyl)-hydroquinone and its derivatives. Phys Chem Chem Phys 17:11990–11999. doi:10.1039/c4cp05651e
11. Harada A, Kobayashi R, Takashima Y et al (2010) Recognition. Nat Chem 3:34–37. doi:10.1038/nchem.893
12. Zhao GJ, Han KL (2008) Effects of hydrogen bonding on tuning photochemistry: concerted hydrogen-bond strengthening and weakening. Chem Phys Chem 9:1842–1846. doi:10.1002/cphc.200800371
13. Gillis EP, Eastman KJ, Hill MD et al (2015) Applications of fluorine in medicinal chemistry. J Med Chem 58:8315–8359. doi:10.1021/acs.jmedchem.5b00258
14. Leroux FR, Manteau B, Vors J-P, Pazenok S (2008) Trifluoromethyl ethers–synthesis and properties of an unusual substituent. Beilstein J Org Chem 4:13. doi:10.3762/bjoc.4.13
15. Shah P, Westwell AD (2007) The role of fluorine in medicinal chemistry. J Enzyme Inhib Med Chem 22:527–540. doi:10.1080/14756360701425014
16. Fluorine in medicinal chemistry and chemical biology—Wiley Online Library. http://onlinelibrary.wiley.com/book/10.1002/9781444312096. Accessed 15 Feb 2016
17. Purser S, Moore PR, Swallow S, Gouverneur V (2008) Fluorine in medicinal chemistry. Chem Soc Rev 37:320–330. doi:10.1039/b610213c
18. Filler R, Saha R (2009) Fluorine in medicinal chemistry: a century of progress and a 60-year retrospective of selected highlights. Future Med Chem 1:777–791. doi:10.4155/fmc.09.65
19. Garcia-Diaz M, Bebenek K (2007) Multiple functions of DNA polymerases. CRC Crit Rev Plant Sci 26:105–122. doi:10.1080/07352680701252817
20. Lu Y, Liu Y, Xu Z et al (2012) Halogen bonding for rational drug design and new drug discovery. Expert Opin Drug Discov 7:375–383. doi:10.1517/17460441.2012.678829
21. Lopachin RM, Gavin T, Decaprio A, Barber DS (2012) Application of the hard and soft, acids and bases (HSAB) theory to toxicant–target interactions. Chem Res Toxicol 25:239–251. doi:10.1021/tx2003257
22. Albà M (2001) Replicative DNA polymerases. Genome Biol 2:REVIEWS3002
23. Lehman IR, Bessman MJ, Simms ES, Kornberg A (1958) Enzymatic synthesis of deoxyribonucleic acid. I. Preparation of

substrates and partial purification of an enzyme from Escherichia coli. J Biol Chem 233:163–170
24. Ollis DL, Brick P, Hamlin R et al (1985) Structure of large fragment of Escherichia coli DNA polymerase I complexed with dTMP. Nature 313:762–766. doi:10.1038/313762a0
25. Allen WJ, Li Y, Waksman G (2010) Bacterial DNA Polymerase I. In: eLS. Wiley, Chichester. doi:10.1002/9780470015902.a0001043.pub2
26. Klenow H, Henningsen I (1970) Selective elimination of the exonuclease activity of the deoxyribonucleic acid polymerase from Escherichia coli B by limited proteolysis. Proc Natl Acad Sci USA 65:168–175
27. Derbyshire V, Grindley ND, Joyce CM (1991) The 3′-5′ exonuclease of DNA polymerase I of *Escherichia coli*: contribution of each amino acid at the active site to the reaction. EMBO J 10:17–24
28. Bernad A, Blanco L, Lázaro J et al (1989) A conserved 3′ → 5′ exonuclease active site in prokaryotic and eukaryotic DNA polymerases. Cell 59:219–228. doi:10.1016/0092-8674(89)90883-0
29. Bhate K, Williams HC (2013) Epidemiology of acne vulgaris. Br J Dermatol 168:474–485. doi:10.1111/bjd.12149
30. Williams HC, Dellavalle RP, Garner S (2012) Acne vulgaris. Lancet 379:361–372. doi:10.1016/S0140-6736(11)60321-8
31. Goodman G (2006) Acne and acne scarring: the case for active and early intervention. Aust Fam Physician 35:503–504
32. Thappa D, Adityan B, Kumari R (2009) Scoring systems in acne vulgaris. Indian J Dermatol Venereol Leprol 75:323. doi:10.4103/0378-6323.51258
33. James WD (2005) Clinical practice. Acne N Engl J Med 352:1463–1472. doi:10.1056/NEJMcp033487
34. Lolis MS, Bowe WP, Shalita AR (2009) Acne and systemic disease. Med Clin North Am 93:1161–1181. doi:10.1016/j.mcna.2009.08.008
35. Titus S, Hodge J (2012) Diagnosis and treatment of acne. Am Fam Physician 86:734–740
36. Fitton A, Goa KL (1991) Azelaic acid. A review of its pharmacological properties and therapeutic efficacy in acne and hyperpigmentary skin disorders. Drugs 41:780–798
37. Azelaic acid (On the skin)—National Library of Medicine—PubMed Health. http://www.ncbi.nlm.nih.gov/pubmedhealth/PMHT0009168/?report=details. Accessed 16 Feb 2016
38. Del Rosso JQ, Baum EW, Draelos ZD et al (2006) Azelaic acid gel 15%: clinical versatility in the treatment of rosacea. Cutis 78:6–19
39. Breathnach AS (1999) Azelaic acid: potential as a general antitumoural agent. Med Hypotheses 52:221–226. doi:10.1054/mehy.1997.0647
40. Graupe K, Cunliffe WJ, Gollnick HP, Zaumseil RP (1996) Efficacy and safety of topical azelaic acid (20 percent cream): an overview of results from European clinical trials and experimental reports. Cutis 57:20–35
41. Bek-Thomsen M, Lomholt HB, Kilian M (2008) Acne is not associated with yet-uncultured bacteria. J Clin Microbiol 46:3355–3360. doi:10.1128/JCM.00799-08
42. Leibl H, Stingl G, Pehamberger H et al (1985) Inhibition of DNA synthesis of melanoma cells by azelaic acid. J Invest Dermatol 85:417–422. doi:10.1111/1523-1747.ep12277084
43. Bojar RA, Holland KT, Cunliffe WJ (1991) The in vitro antimicrobial effects of zelaic acid upon Propionibacterium acnes strain P37. J Antimicrob Chemother 28:843–853
44. Gleeson MP, Gleeson D (2009) QM/MM calculations in drug discovery: a useful method for studying binding phenomena? J Chem Inf Model 49:670–677. doi:10.1021/ci800419j
45. Becke AD (1988) Density-functional exchange-energy approximation with correct asymptotic behavior. Phys Rev A 38:3098–3100. doi:10.1103/PhysRevA.38.3098
46. Lee C, Yang W, Parr RG (1988) Development of the Colle-Salvetti correlation-energy formula into a functional of the electron density. Phys Rev B 37:785–789. doi:10.1103/PhysRevB.37.785
47. Frisch MJ, Trucks GW, Schlegel HB et al (2009) Gaussian 09, Revision A.02. Gaussian Inc Wallingford CT 34, Wallingford CT. doi:10.1159/000348293
48. Ray SS, Bonanno JB, Rajashankar KR et al (2002) Cocrystal structures of diaminopimelate decarboxylase: mechanism, evolution, and inhibition of an antibiotic resistance accessory factor. Structure 10:1499–1508. doi:10.1016/S0969-2126(02)00880-8
49. Parr RG, Yang W (1989) Density-functional theory of atoms and molecules. Int J Quantum Chem. doi:10.1002/qua.560470107
50. Pearson RG (1995) The HSAB principle—more quantitative aspects. Inorg Chim Acta 240:93–98. doi:10.1016/0020-1693(95)04648-8
51. Pearson RG (1986) Absolute electronegativity and hardness correlated with molecular orbital theory. Proc Natl Acad Sci USA 83:8440–8441. doi:10.1073/pnas.83.22.8440
52. Brautigam CA, Sun S, Piccirilli JA, Steitz TA (1999) Structures of normal single-stranded DNA and deoxyribo-3′-S-phosphorothiolates bound to the 3′-5′ exonucleolytic active site of DNA polymerase I from Escherichia coli. Biochemistry 38:696–704. doi:10.1021/bi981537g
53. Guex N, Peitsch MC (1997) SWISS-MODEL and the Swiss-PDBVIEWER: an environment for comparative protein modeling. Electrophoresis 18:2714–2723. doi:10.1002/elps.1150181505
54. Dundas J, Ouyang Z, Tseng J et al (2006) CASTp: computed atlas of surface topography of proteins with structural and topographical mapping of functionally annotated residues. Nucleic Acids Res 34:116–118. doi:10.1093/nar/gkl282
55. DeLano WL (2002) The PyMOL molecular graphics system. Schrödinger LLC wwwpymolorg Version 1.:http://www.pymol.org. doi: citeulike-article-id:240061
56. Trott O, Olson AJ (2010) Software news and update AutoDock Vina: improving the speed and accuracy of docking with a new scoring function, efficient optimization, and multithreading. J Comput Chem 31:455–461. doi:10.1002/jcc.21334
57. Morris GM, Lim-Wilby M (2008) Molecular docking. Methods Mol Biol 443:365–382. doi:10.1007/978-1-59745-177-2_19
58. Trott O, Olson AJ (2010) AutoDock Vina. J Comput Chem 31:445–461. doi:10.1002/jcc.21334
59. Updated L (2013) Accelrys discovery studio 4.0 product release document
60. Laskowski RA, Swindells MB (2011) LigPlot+: multiple ligand-protein interaction diagrams for drug discovery. J Chem Inf Model 51:2778–2786. doi:10.1021/ci200227u
61. Cheng F, Li W, Zhou Y et al (2012) AdmetSAR: a comprehensive source and free tool for assessment of chemical ADMET properties. J Chem Inf Model 52:3099–3105. doi:10.1021/ci300367a
62. Garbett NC, Chaires JB (2012) Thermodynamic studies for drug design and screening. Expert Opin Drug Discov 7:299–314. doi:10.1517/17460441.2012.666235
63. Lien EJ, Guo Z-R, Li R-L, Su C-T (1982) Use of dipole moment as a parameter in drug-receptor interaction and quantitative structure-activity relationship studies. J Pharm Sci 71:641–655. doi:10.1002/jps.2600710611
64. Lien EJ, Guo ZR, Li RL, Su CT (1982) Use of dipole moment as a parameter in drug-receptor interaction and quantitative structure–activity relationship studies. J Pharm Sci 71:641–655
65. Rahman A, Hoque MM, Khan MAK et al (2016) Non-covalent interactions involving halogenated derivatives of capecitabine and thymidylate synthase: a computational approach. Springerplus 5:1–18. doi:10.1186/s40064-016-1844-y

66. Saleh MA, Solayman M, Hoque MM et al (2016) Inhibition of DNA topoisomerase type IIα (TOP2A) by Mitoxantrone and its halogenated derivatives: a combined density functional and molecular docking study. Biomed Res Int 2016:12
67. Heinz H, Suter UW (2004) Atomic charges for classical simulations of polar systems. J Phys Chem B 108:18341–18352. doi:10.1021/jp048142t
68. Gross KC, Seybold PG, Hadad CM (2002) Comparison of different atomic charge schemes for predicting pKa variations in substituted anilines and phenols. Int J Quantum Chem 90:445–458. doi:10.1002/qua.10108
69. Fukui K, Yonezawa T, Shingu H (1952) A molecular orbital theory of reactivity in aromatic hydrocarbons. J Chem Phys 20:722. doi:10.1063/1.1700523
70. Ayers PW, Parr RG, Pearson RG (2006) Elucidating the hard/soft acid/base principle: a perspective based on half-reactions. J Chem Phys 124:194107. doi:10.1063/1.2196882
71. Parr RG, Zhou Z (1993) Absolute hardness : unifying concept for identifying shells and subshells in nuclei, atoms, molecules, and metallic clusters. Acc Chem Res 26:256–258. doi:10.1021/ar00029a005
72. Aihara J (1999) Reduced HOMO-LUMO gap as an index of kinetic stability for polycyclic aromatic hydrocarbons. J Phys Chem A 103:7487–7495. doi:10.1021/jp990092i
73. Manolopoulos DE, May JC, Down SE (1991) Theoretical studies of the fullerenes: c34 to C70. Chem Phys Lett 181:105–111. doi:10.1016/0009-2614(91)90340-F
74. Aihara J (2000) Correlation found between the HOMO–LUMO energy separation and the chemical reactivity at the most reactive site for isolated-pentagon isomers of fullerenes. Phys Chem Chem Phys 2:3121–3125. doi:10.1039/b002601h
75. Gelb MH, Svaren JP, Abeles RH (1985) Fluoro ketone inhibitors of hydrolytic enzymes. Biochemistry 24:1813–1817. doi:10.1021/bi00329a001
76. Nair HK, Quinn DM (1993) M-alkyl alpha, alpha, alpha-trifluoroacetophenones—a new class of potent transition-state analog inhibitors of acetylcholinesterase. Bioorg Med Chem Lett 3:2619–2622. doi:10.1016/S0960-894x(01)80727-7
77. Veale CA, Bernstein PR, Bohnert CM et al (1997) Orally active trifluoromethyl ketone inhibitors of human leukocyte elastase. J Med Chem 40:3173–3181. doi:10.1021/jm970250z
78. Furuya T, Kamlet AS, Ritter T (2011) Catalysis for fluorination and trifluoromethylation. Nature 473:470–477. doi:10.1038/nature10108
79. McClinton MA, McClinton DA (1992) Trifluoromethylations and related reactions in organic chemistry. Tetrahedron 48:6555–6666. doi:10.1016/S0040-4020(01)80011-9
80. Ji Y, Brueckl T, Baxter RD et al (2011) Innate C–H trifluoromethylation of heterocycles. Proc Natl Acad Sci USA 108:14411–14415. doi:10.1073/pnas.1109059108
81. Lishchynskyi A, Novikov MA, Martin E et al (2013) Trifluoromethylation of aryl and heteroaryl halides with fluoroform-derived CuCF3: scope, limitations, and mechanistic features. J Org Chem 78:11126–11146. doi:10.1021/jo401423h
82. Sarwar MG, Ajami D, Theodorakopoulos G et al (2013) Amplified halogen bonding in a small space. J Am Chem Soc 135:13672–13675. doi:10.1021/ja407815t
83. Sarwar MG, Dragisic B, Salsberg LJ et al (2010) Thermodynamics of halogen bonding in solution: substituent, structural, and solvent effects. J Am Chem Soc 132:1646–1653. doi:10.1021/ja9086352
84. Beale TM, Chudzinski MG, Sarwar MG, Taylor MS (2013) Halogen bonding in solution: thermodynamics and applications. Chem Soc Rev. doi:10.1039/c2cs35213c
85. Hoque MM, Halim MA, Rahman MM et al (2013) Synthesis and structural insights of substituted 2-iodoacetanilides and 2-iodoanilines. J Mol Struct 1054–1055:367–374. doi:10.1016/j.molstruc.2013.10.011
86. Sarwar MG, Dragisić B, Dimitrijević E, Taylor MS (2013) Halogen bonding between anions and iodoperfluoroorganics: solution-phase thermodynamics and multidentate-receptor design. Chem A Eur J 19:2050–2058. doi:10.1002/chem.201202689
87. Sarwar MG, Dragisic B, Sagoo S, Taylor MS (2010) A tridentate halogen-bonding receptor for tight binding of halide anions. Angew Chem Int Ed Engl 49:1674–1677. doi:10.1002/anie.200906488
88. Bissantz C, Kuhn B, Stahl M (2010) A medicinal chemist's guide to molecular interactions. J Med Chem 53:5061–5084. doi:10.1021/jm100112j
89. Hunter CA (2004) Quantifying intermolecular interactions: guidelines for the molecular recognition toolbox. Angew Chemie Int Ed 43:5310–5324. doi:10.1002/anie.200301739
90. Zhurkin VB, Tolstorukov MY, Xu F et al (2005) Sequence-dependent variability of B-DNA. DNA conform transcription. Springer, Boston, pp 18–34
91. Wade RC, Goodford PJ (1989) The role of hydrogen-bonds in drug binding. Prog Clin Biol Res 289:433–444
92. Zhao GJ, Liu JY, Zhou LC, Han KL (2007) Site-selective photoinduced electron transfer from alcoholic solvents to the chromophore facilitated by hydrogen bonding: a new fluorescence quenching mechanism. J Phys Chem B 111:8940–8945. doi:10.1021/jp0734530
93. Zhao G-J, Han K-L (2008) Site-specific solvation of the photoexcited protochlorophyllide a in methanol: formation of the hydrogen-bonded intermediate state induced by hydrogen-bond strengthening. Biophys J 94:38–46. doi:10.1529/biophysj.107.113738
94. Lee HR, Helquist SA, Kool ET, Johnson KA (2008) Importance of hydrogen bonding for efficiency and specificity of the human mitochondrial DNA polymerase. J Biol Chem 283:14402–14410. doi:10.1074/jbc.M705007200
95. Derbyshire V, Freemont PS, Sanderson MR et al (1988) Genetic and crystallographic studies of the 3′,5′-exonucleolytic site of DNA polymerase I. Science 240:199–201
96. Kuduva SS, Craig DC, Nangia A, Desiraju GR (1999) Cubanecarboxylic acids. Crystal engineering considerations and the role of C-H···O hydrogen bonds in determining O-H···O networks. J Am Chem Soc 121:1936–1944. doi:10.1021/ja981967u
97. Meadows ES, De Wall SL, Barbour LJ et al (2000) Structural and dynamic evidence for C − H···O hydrogen bonding in lariat ethers: implications for protein structure. J Am Chem Soc 122:3325–3335. doi:10.1021/ja9940672
98. Amin ML (2013) P-glycoprotein inhibition for optimal drug delivery. Drug Target Insights 2013:27–34. doi:10.4137/DTI.S12519
99. Sanguinetti MC, Tristani-Firouzi M (2006) hERG potassium channels and cardiac arrhythmia. Nature 440:463–469. doi:10.1038/nature04710